

# Associations between the Structure of Urban Landscape and Particulate Matter: A STURLA Case Study in Philadelphia, PA

Lucas E. Cummings<sup>\*1</sup>, Justin D. Stewart<sup>\*1,2</sup>, Peleg Kremer<sup>1</sup>, Kabindra.M. Shakya<sup>1</sup>

<sup>\*</sup>These authors contributed to this work equally

<sup>1</sup>Department of Geography and the Environment, Villanova University, Pennsylvania, USA

<sup>2</sup>Department of Ecological Science, Vrije Universiteit Amsterdam, 1081 HV Amsterdam, The Netherlands

## **Corresponding author**

Peleg Kremer  
800 Lancaster Avenue, Villanova, PA 19085, USA  
Department of Geography & the Environment  
Villanova University  
Phone: 610-519-3590  
Email: [peleg.kremer@villanova.edu](mailto:peleg.kremer@villanova.edu)

## **Author Contributions**

Conceptualization: KMS, PK. Data Collection: JDS, KMS, PK. Formal Data Analysis: JDS, LEC. Writing: LEC, JDS, KMS, PK. Supervision & Funding Acquisition: KMS, PK

## **ORCID:**

LEC: 0000-0002-7685-0525  
JDS: 0000-0002-7812-5095  
PK: 0000-0001-6844-5557  
KMS: 0000-0002-7035-7019

Sources of Support: NSF Grant # [1832407](#)

Data Availability:

Word count:

## **Acknowledgements**

We would like to thank Meghan Conway, Radley Reist, and Alexander Saad for their assistance in data collection. Financial support for this study was provided through National Science Foundation (NSF) grant #1832407.

## **Declaration of Interest**

The authors declare that there is no conflict of interest.

**Abstract:**

Understanding the relationships between land cover/urban structure patterns and air pollutants is key to sustainable urban planning and development. In this study, we employ a mobile monitoring method to collect PM<sub>2.5</sub> and BC data in the city of Philadelphia, PA during the summer of 2019 and apply the Structure of Urban Landscapes (STURLA) methodology to examine relationships between urban structure and atmospheric pollution. We find that, while PM<sub>2.5</sub> and BC vary by STURLA class, many of the differences in pollutant concentrations between classes are not significant. However, we also find that the proportions in which STURLA components are present throughout the urban landscape can be used to predict urban air pollution. Among frequently sampled STURLA classes, *gpl* hosted the highest PM<sub>2.5</sub> concentrations on average ( $16.60 \pm 4.29 \mu\text{g}/\text{m}^3$ ), while *tgbwp* hosted the highest BC concentrations ( $2.31 \pm 1.94 \mu\text{g}/\text{m}^3$ ). Furthermore, STURLA combined with machine learning modeling was able to correlate PM<sub>2.5</sub> ( $R^2 = 0.68$ , RMSE  $2.82 \mu\text{g}/\text{m}^3$ ) and BC ( $R^2 = 0.64$ , RMSE  $0.75 \mu\text{g}/\text{m}^3$ ) concentrations with the urban landscape and spatially interpolate concentrations where sampling did not take place. These results demonstrate the efficacy of the STURLA methodology in modeling relationships between air pollution and land cover/urban structure patterns.

**1.0 Introduction:**

Population growth in urban areas is increasing rapidly; the United Nations projects that 68% of the world's population will live in urban areas by 2050 (UN DESA, 2018). As urban areas expand, a larger proportion of the global population will be exposed to increasingly high and potentially harmful levels of air pollution. At present, 9 out of 10 people regularly breathe air containing unsafe level of air pollutants (WHO, 2018), and approximately 3.7 million premature deaths worldwide can be attributed to elevated air pollutant concentrations each year (Cohen et al., 2017). Elevated levels of air pollutants disproportionately impact people based on race, (Perlin et al. 1999; Perlin et al. 2001; Gray et al. 2013), gender and sexual orientation (Collins et al., 2017) and socioeconomic status (Perlin et al. 1999; Zhou et al. 2011; Gray et al. 2013). To ensure that air quality management is equitable and protects the health of urban populations, it is crucial that we understand how air pollutants interact with the urban environment.

Particulate matter (PM) has been linked to negative health outcomes, including asthma (Halonen et al., 2008; Anenberg et al. 2018), lung cancer (Hamra et al. 2014; Pope et al. 2002), DNA alteration (Sorensen et al. 2003; Shi et al., 2019; Baccarelli et al., 2009), and disrupted immune function (Zelikoff et al., 2008; Honda et al. 2017). Polluted airs also host potentially pathogenic bacteria (Stewart et al., 2020; Liu et al., 2018) and viruses (Wu et al., 2020; Zhu et al., 2020) that may cause disease and aggravate pre-existing conditions. Fine particulate matter (PM<sub>2.5</sub>) is of significant concern due to its abundance in urban atmospheres, and subsequent potential to cause respiratory and cardiovascular damage (Dockery et al., 1993; Paul et al., 2019; Rabinovitch et al., 2006; Shakya et al., 2016). Black carbon (BC), a subset of PM<sub>2.5</sub>, is generated through incomplete combustion of fossil fuels and is particularly prevalent in urban areas. Unlike PM<sub>2.5</sub>, almost all of BC originates from anthropogenic sources, with biomass fires being the only natural source of BC (Hitzenberger & Tohno, 2001); as

such, BC is commonly used as an indicator of anthropogenic influence on ambient air pollution (Cyrus et al., 2003; Targino et al., 2016).

Studies of urban air pollution have established relationships between land cover, urban structure, and ambient air pollution (Eeftens et al. 2012; Yuan et al. 2019). In urban areas such as Philadelphia, particulate matter concentrations vary across neighborhoods as a result of differences in open space and land structure (Shakya et al., 2019). The organization and height of buildings, barriers and other structures in an urban environment can influence air flow, which in turn impacts local pollutant dispersal (Baldauf et al., 2016; Gallagher et al., 2015; Ng & Chau, 2013; Yang et al., 2020). Though many urban areas are characterized by dense built environment, different types of urban green space (e.g. urban forest, parks, gardens, and private yards) are an integral part of the urban landscape. Over the last few decades, cities are increasingly adopting strategies such as urban greening to counteract environmental degradation and enhance human wellbeing. However, these strategies and their efficacy in mitigating urban air pollution are still unclear (Nemitz et al., 2020). While vegetation such as trees and grasses have been shown to reduce air pollution by facilitating pollutant deposition and uptake of particulate matter, they are also capable of causing an increase in local pollutant concentrations through biogenic emissions that serve to facilitate secondary aerosol formation and the inhibition of air flow (Brantley et al. 2014; Chen et al. 2016; Eisenman et al. 2019; Xing & Brimblecombe 2019).

Although it is becoming increasingly clear how individual components of urban environments influence air pollution, complex urban topologies make it difficult to understand how these individual components interact to influence air pollution at more localized scales. In urban environments, land cover and urban structures often change drastically over short distances (Cadenasso et al., 2007). While cities may contain common environmental features such as water and greenspace, differences in their organization have varied impacts on air quality, further complicating efforts to generalize the impact that urban environments have on air pollution. Thus, sustainable development is contingent on reproducible and scalable analyses that geographically meaningful units for urban planning and development. To this end, there have been efforts to streamline the characterization of cities at smaller scales. The Structure of Urban Landscape (STURLA) composite classification allows for modeling of three-dimensional urban areas at fine spatial scales. STURLA does so by using fine-scale land cover and building height data to identify common compositions of urban environments (Hamstead et al., 2016). STURLA studies have linked urban landscape structure and land surface temperature (Hamstead et al., 2016; Kremer et al. 2018; Larondelle et al., 2014; Mitz et al., 2021), as well as the phylogenetic diversity of the atmospheric microbiome (Stewart et al. 2021). STURLA allows for meaningful classifications of urban structure and land cover, which have the potential to reshape our understanding of how the composition and spatial organization of urban environments influence environmental parameters. There have also been efforts to improve the accuracy of urban air pollution measurement, as variability in urban landscape composition can influence pollutant dispersal and affect concentrations at small scales (Abhijith & Gokhale, 2015; Gallagher et al. 2015; Hagler et al., 2012). In recent years, mobile monitoring has emerged as a novel method with which to study the spatiotemporal distribution of air pollutants in urban environments (Apte et al., 2017;

deSouza et al., 2020; Deville Cavellin et al., 2016; Shakya et al., 2019; Sm et al., 2019; Targino et al., 2016; Van Poppel et al., 2013), as it can collect data at finer spatial scales than is feasible with stationary monitoring (Shakya et al., 2019; Van den Bossche et al., 2015) and does not rely on interpolation to characterize pollutants throughout a city. In this study, we use data collected through mobile monitoring to measure concentrations of particulate matter smaller than 2.5  $\mu\text{m}$  ( $\text{PM}_{2.5}$ ) and black carbon (BC) throughout the city of Philadelphia over the course of 12 days during the summer of 2019 (Cummings & Stewart et al., 2021, preprint). We use STURLA (Hamstead et al., 2016) in conjunction with the collected air pollution data to analyze the urban structure-air pollution relationship across the city of Philadelphia.

## 2.0 Methods

### 2.1 Site Description

Philadelphia, Pennsylvania is the sixth-most populous city in the United States of America and the largest city in the state of Pennsylvania, with an estimated population of 1,584,138 residents in 2018. Philadelphia is a northeastern U.S. city defined by a dense urban core surrounded by predominantly low-rise residential and commercial districts, city parks, and industrial sectors. Two major rivers flow through the city: the Delaware River, which flows southward into the Delaware Bay and Atlantic Ocean, and the Schuylkill River, which flows southward through the western neighborhoods of Philadelphia. The southern and eastern parts of the city house heavy industry along both riverbanks, while large park areas are found in the western and northern areas of the city. For planning purposes, Philadelphia is divided into 18 different planning districts (Figure 1, Table A1).

### 2.2 Philadelphia STURLA

The STURLA profile for Philadelphia was made by joining land cover raster data and building height data from 2017 as in Stewart et al. 2021 (Figure 1). A fishnet with 120m<sup>2</sup> pixels was overlaid on the joined land cover / building height raster. STURLA classifications for each cell were determined based on the presence of each land cover / urban structure component identified; each letter in the STURLA code represents a different component of the urban environment. Each color within a given pixel color within a STURLA cell indicates a specific combination of different urban structure components: trees (t), grass (g), bare soil (b), water (w), pavement (p), low-rise buildings (1 – 3 stories) (l), mid-rise buildings (4 – 9 stories) (m), and/or high-rise buildings (9+ stories) (h). Philadelphia contains 86 STURLA classes, although most of the city can be characterized by just a few classes; *tgpl* is by far the most common class, describing about 51.7% of Philadelphia. Other common classes include *tgplm*, *tgp*, *tgbpl*, *tgwp*, and *w* (Figure 1). Letters in the STURLA class code denote the presence of specific features of the urban landscape (Figure 2).

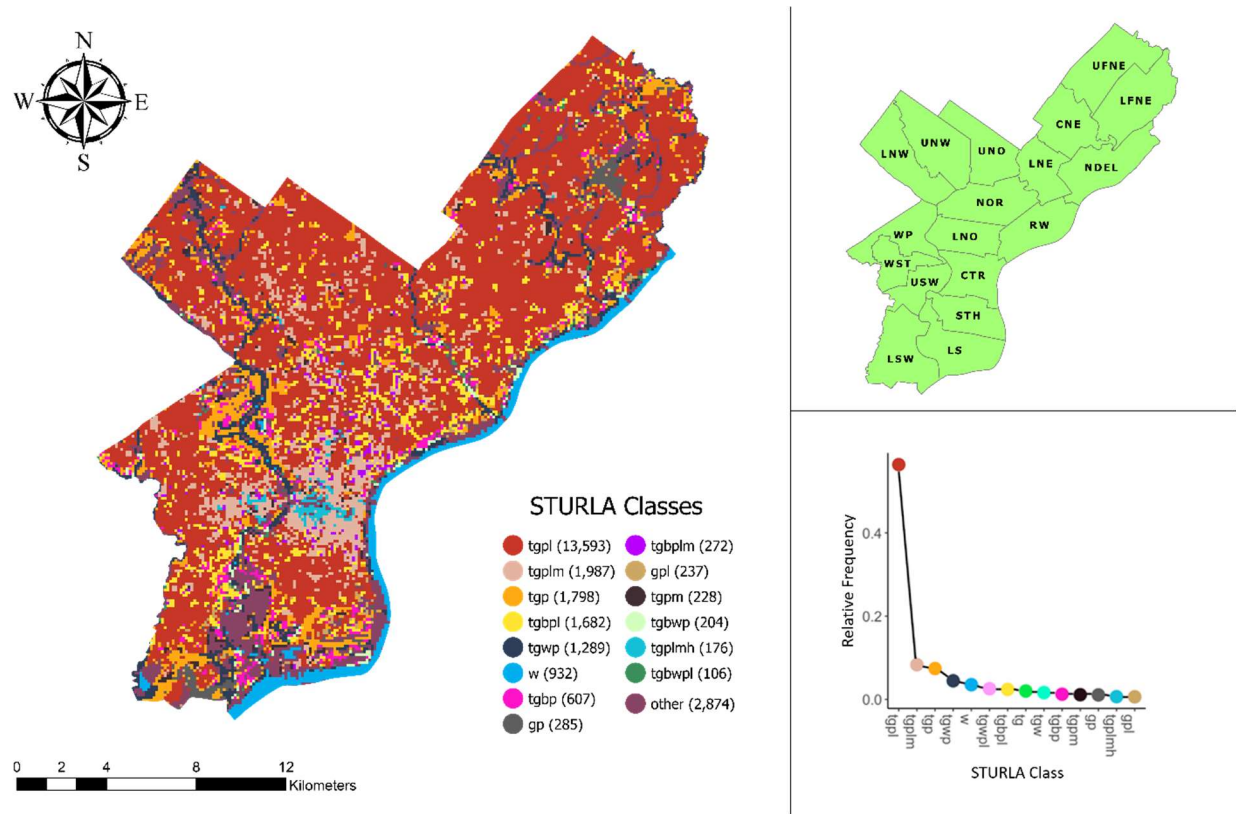


**Figure 1.** Map of STURLA classes in Philadelphia, Pennsylvania (left). Classes symbolized include the 14 most sampled classes, which make up 85.5% of Philadelphia; w is also included for representation of major waterways. The “other” class consists of the other 72 classes found throughout Philadelphia which, with water, characterize the remaining 14.5% of the city. Also included are Philadelphia’s planning zones (top-right) and a ranked abundance plot (bottom-right) showing relative frequencies of the 14 most abundant STURLA classes throughout Philadelphia.



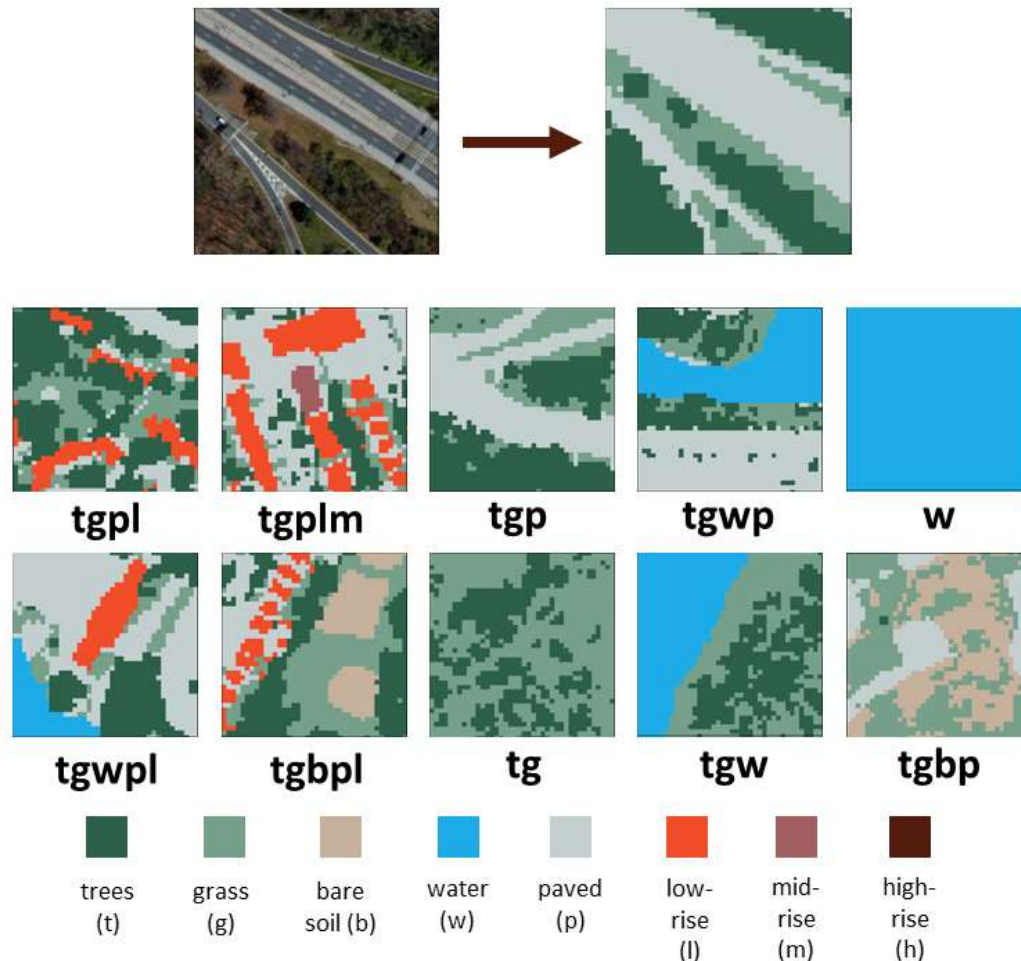


**Figure 2.** Examples of pixels of common STURLA classes symbolized on a land cover/building height data raster. Each color within a STURLA cell indicates the presence of a different urban structure component: trees (*t*), grass (*g*), bare soil (*b*), water (*w*), pavement (*p*), low-rise buildings (1 – 3 stories) (*l*), mid-rise buildings (4 – 9 stories) (*m*), and high-rise buildings (9+ stories) (*h*).

### 2.3 Sampling Description

PM<sub>2.5</sub> and BC data were collected using a mobile monitoring method. A van, equipped with instrumentation measuring geolocation data (Trimble Juno 3B with Trimble R1 GNSS receivers), PM<sub>2.5</sub> concentrations (Grimm Portable Laser Aerosol Spectrometer, Model 11-C), and BC concentrations (MicroAeth MA200) was driven along two predetermined routes in Philadelphia. Sampling equipment was set up and calibrated as described in Cummings & Stewart et al. 2021 (preprint). Data was captured at different temporal resolutions; GPS data was recorded at every one second interval, BC data was recorded at every five second interval, and PM data was recorded at every six second interval (Table A2).

Driving routes were determined using a stratified random sample of STURLA cells in order to ensure that a representative sample of Philadelphia's STURLA class

distribution was captured during the sampling period (Figure A1). Specific points of interest such as United States Environmental Protection Agency (U.S. EPA) Toxics Release Inventory (TRI) sites, EPA air pollution monitoring station sites, the Philadelphia Water Department's green infrastructure sites, and census tracts with high rates of asthma were also considered in route development. An optimized ~483 km (300 mile) driving route that took STURLA class distribution and points of interest into account was generated using Network Analyst in ArcGIS 10.7.1. This optimized route was divided into two ~241.5 km (150 mile) segments in order to make the routes drivable within a day. Occasional road closures in Philadelphia created slight variability in the routes traveled from day to day.

Sampling occurred over a period of 12 days between June 27 and July 29, 2019; each route was sampled six times. Sampling occurred on days where inclement weather (i.e. rain) did not pose a risk to the monitoring equipment; as such, weather conditions during the sampling days were similar (Table A3). Sampling began between 6 – 7 AM on one of the two routes and continued until the entirety of the route was traveled; the sampling period on any given day ranged from about 8 hours to 10.5 hours. Vehicle speed averaged ~20 km/hr throughout the data collection period.

## 2.4 Data Analysis

Air pollution and geolocation data were joined by time. For each day of data collection, air pollution data was spatially joined to Philadelphia's STURLA profile in ArcGIS Pro 2.4; each pixel was assigned the value of the average concentration of all points that fell within it. All cells that contained at least one point were selected and summarized to obtain the average concentration for each STURLA class. The mean concentrations for each class on each day were averaged to determine an average daily mean concentration for each STURLA class for which at least 20 unique cells were sampled; classes that were sampled in fewer than 20 unique cells were summarized into an "other" class for which daily averages were calculated. Permutational t-tests (number of permutations = 10,000) from the "RVAidemoire" package in R were used to determine if differences in the daily mean air pollutant concentrations of STURLA classes were significant, as they take varying sample sizes into account (Hervé 2020). For each class sampled, the composition of an average cell was determined by finding the mean percentage of all land cover / urban structure components for each cell sampled belonging to a specific class. Differences in average STURLA class composition were evaluated using hierarchical clustering based on Bray-Curtis dissimilarities between classes. The clustering dendrogram (Figure 3) demonstrates compositional similarities between classes; classes with fewer branches separating them are more similar to each other than those with more branches separating them.

A supervised machine learning model, Random Forest Regression, was used to investigate the possible distribution of PM<sub>2.5</sub> and BC in areas not sampled based on measured concentrations and the STURLA landscape components in sampled areas. This method uses an ensemble of weak models that draw a random sample from the original dataset and splits them into a forest of decision trees, which helps to account for spatial autocorrelation and non-linear relationships more effectively than linear models (Oliveira, 2012). Using the "caret" package (Kuhn et al. 2008) in R (3.3.6) (Ihaka &

Gentleman, 1996) data were split into 60% training and 40% validation sets that underwent 10-fold cross-validation. The model was trained using the average within-class STURLA land cover / urban structure percentages for each class and the mean pollutant concentration measured in that class (e.g. class *tgpl* is the supervised label attached to the mean landscape percentages for *tgpl* across Philadelphia). Root Mean Standard Error (RMSE) was used to assess model error. We define validation error as the ratio of predicted to measured concentrations. Variable importance is measured as the percent increase in RMSE by removing a variable from the model where once completed for each variable is ranked. Model predictions and results were joined by STURLA class and visualized using ArcMap 10.7.1.

### 3.0 Results

#### 3.1 Variation in Landscape Structure with $PM_{2.5}$ and BC Concentrations Among STURLA Classes

Differences in both landscape composition and the measured pollutant concentrations they host are evident among the most sampled STURLA classes (Figure 3). Although a slightly different subset of cells was sampled for  $PM_{2.5}$  and BC due to differences in temporal resolutions of sampling equipment (5 seconds for BC compared to 6 seconds for  $PM_{2.5}$ ), differences in average STURLA class composition are minimal and did not influence clustering between classes. Daily means for  $PM_{2.5}$  among STURLA classes range from  $11.47 \pm 1.89 \mu\text{g}/\text{m}^3$  (*tgbplm*) to  $16.60 \pm 4.29 \mu\text{g}/\text{m}^3$  (*gpl*), while daily means for BC range from  $1.25 \pm 0.71 \mu\text{g}/\text{m}^3$  (*tgbplm*) to  $2.31 \pm 1.94 \mu\text{g}/\text{m}^3$  (*tgbwp*) (Figure 3). Permutational t-tests reveal that some of the differences in pollutant concentrations between STURLA classes are statistically significant ( $p < 0.05$ ) (Figure 4). Class *gpl* demonstrated the most unique  $PM_{2.5}$  signature, with daily mean  $PM_{2.5}$  concentrations differing significantly from six classes: *tgp*, *tgplm*, *tgwp*, *tgpm*, *tgbplm*, and *tgplmh*. Class *tgbplm* presented the most distinct BC signature with the daily average BC concentration being significantly different from four other classes sampled: *tgplmh*, *gpl*, *tgbwp*, and *gp*. However, other STURLA classes did not have pollutant concentrations that were significantly different from other classes. More significant differences between classes were found with  $PM_{2.5}$  concentrations (17) than with BC concentrations (9) (Figure 4).



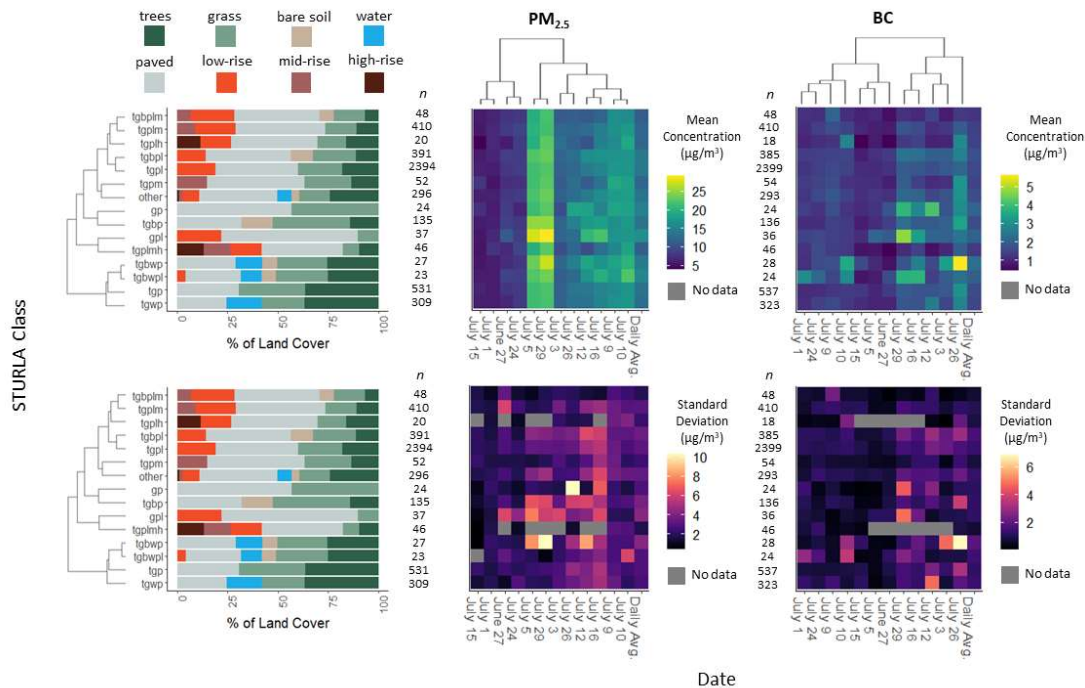


**Figure 3.** Composition of the average cell sampled for each class (left), sample sizes, and daily/overall means and standard deviations of measured PM<sub>2.5</sub> (middle) and BC (right) concentrations. Overall means are represented in the top heatmaps, while standard deviations are represented in the bottom heatmaps; darker colors (blue, purple) represent lower concentrations and lighter colors (yellow) represent higher concentrations. Dendrograms reflect similarities in pollutant concentrations between days (top) and STURLA class composition (left).

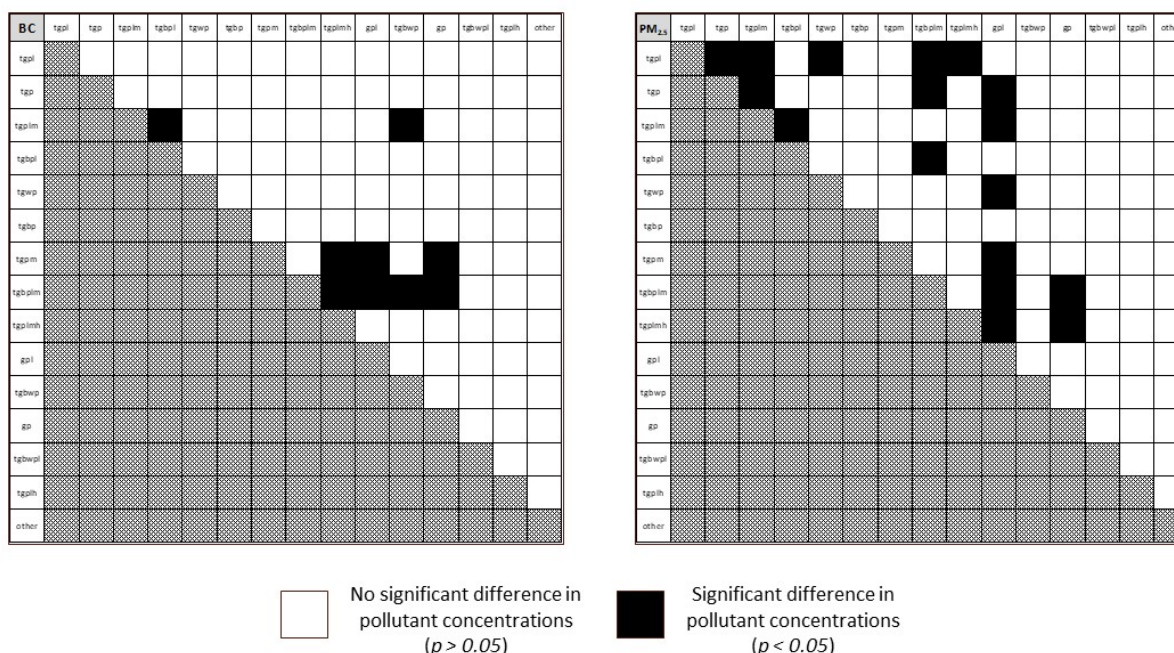


**Figure 4.** Results of pairwise permutational t-tests between STURLA classes comparing average daily pollutant concentrations for BC (left) and PM<sub>2.5</sub> (right). Black cells indicate significant differences in pollutant concentrations between classes.

### 3.2 Spatial Modeling of PM<sub>2.5</sub> and BC

Pavement was the most important variable in modeling PM<sub>2.5</sub>, followed by high-rise, grass, trees, mid-rise, water, and low-rise (Figure 5A). In modeling BC, low-rise was the most important variable, followed by pavement, trees, grass, mid-rise, high-rise, and water (Figure 5E). In both models, bare soil did not contribute to predictions of pollutant concentrations (Figure 5A, 5E). Predictions varied by STURLA class (Figure 5B, 5F). Philadelphia's most frequent class, *ttpl*, has a mean prediction of 13.71  $\mu\text{g}/\text{m}^3$ ; modeling overpredicted the average measured concentration of the class by 1.64  $\mu\text{g}/\text{m}^3$ . STURLA classes *gpb*, *ttp*, and *gpl* are among the classes with the highest predicted concentrations, while *pm*, *ttwpl*, *gwp* had the lowest (Supplemental Table 1). Variation in PM<sub>2.5</sub> concentrations across the city were largely explained by differences in sampled STURLA classes ( $R^2 = 0.68$ , RMSE 1.10  $\mu\text{g}/\text{m}^3$ ). PM<sub>2.5</sub> predictions ranged from 8.77 – 15.29  $\mu\text{g}/\text{m}^3$ ; actual PM<sub>2.5</sub> concentrations by class ranged from 5.40 – 22.21  $\mu\text{g}/\text{m}^3$ . Differences between STURLA class composition were slightly less effective in explaining variation in BC concentrations ( $R^2 = 0.64$ , RMSE 0.91  $\mu\text{g}/\text{m}^3$ ). BC predictions by class were generally higher than measured concentrations (Figure 5G), and ranged from 1.26  $\mu\text{g}/\text{m}^3$  to 3.76  $\mu\text{g}/\text{m}^3$  (Figure 5F); actual concentrations by class ranged from 0.85 – 5.45  $\mu\text{g}/\text{m}^3$ . BC predictions in *ttpl* hosted predicted BC values of 1.65  $\mu\text{g}/\text{m}^3$  and overpredicted measured BC in *ttpl* pixels by 0.07  $\mu\text{g}/\text{m}^3$ . Classes *tpl*, *tp*, and *ttwpm* were the classes with the highest BC predictions, while *ttbph*, *ttplmh*, and *ttbplh* had the lowest predictions (Figure 5G).

**Table 1.** Summary of measured pollutant concentrations, predicted pollutant concentrations, differences between predicted and measured, and validation error by Philadelphia planning district.

Planning District	Mean Predicted PM <sub>2.5</sub>	Mean Measured PM <sub>2.5</sub>	P – M (PM <sub>2.5</sub> )	Validation Error	Mean Predicted BC	Mean Measured BC	P – M (BC)	Validation Error
Central	12.62	12.74	-0.12	0.994	1.54	1.49	0.05	1.040
Central Northeast	13.60	13.88	-0.28	0.981	1.65	1.57	0.08	1.062
Lower Far Northeast	13.74	14.11	-0.37	0.975	1.68	1.63	0.05	1.046
Lower North	13.40	13.55	-0.15	0.991	1.62	1.56	0.06	1.040
Lower Northeast	13.71	14.03	-0.32	0.978	1.65	1.59	0.06	1.040
Lower Northwest	13.59	13.83	-0.24	0.984	1.64	1.55	0.09	1.078
Lower South	12.83	12.85	0.02	1.036	1.78	1.66	0.12	1.134
Lower Southwest	13.59	13.84	-0.25	0.988	1.72	1.65	0.07	1.069
North	13.54	13.75	-0.21	0.986	1.64	1.59	0.05	1.036
North Delaware	13.73	14.01	-0.28	0.983	1.70	1.65	0.05	1.038
River Wards	13.63	13.85	-0.22	0.988	1.71	1.66	0.05	1.052
South	13.56	13.94	-0.38	0.975	1.68	1.62	0.06	1.043
University Southwest	13.20	13.38	-0.18	0.989	1.61	1.56	0.05	1.037
Upper Far Northeast	13.74	14.09	-0.35	0.976	1.66	1.60	0.06	1.047
Upper North	13.62	13.95	-0.33	0.976	1.65	1.58	0.07	1.044
Upper Northwest	13.55	13.85	-0.30	0.979	1.64	1.57	0.07	1.049
West	13.58	13.88	-0.30	0.979	1.64	1.57	0.07	1.040
West Park	13.53	13.60	-0.07	0.997	1.67	1.59	0.08	1.057

PM<sub>2.5</sub> predictions by planning district ranged from 12.62 µg/m<sup>3</sup> – 13.74 µg/m<sup>3</sup>; the highest predicted PM<sub>2.5</sub> concentrations are in the Upper Far Northeast and Lower Far Northeast planning districts, while the lowest predicted concentrations were found in the Central planning district (Table 1). 17 of 18 planning districts underpredicted measured PM<sub>2.5</sub> concentrations (Predicted PM<sub>2.5</sub> / Measured PM<sub>2.5</sub> ratio < 1), which ranged from 12.74 µg/m<sup>3</sup> – 14.11 µg/m<sup>3</sup> (Table 1). PM<sub>2.5</sub> modeling was the most accurate in the Lower South district, with a difference of 0.02 µg/m<sup>3</sup> between predicted and measured concentrations, but least accurate in the South district, with a 0.38 µg/m<sup>3</sup> difference between predicted and measured concentrations. Conversely, the model overpredicted BC concentrations in all 18 planning districts, and generally overpredicted BC

concentrations by STURLA class (Table 1, Figure 5G). Predicted BC concentrations ranged from  $1.54 \mu\text{g}/\text{m}^3$  –  $1.78 \mu\text{g}/\text{m}^3$ , while measured BC concentrations ranged from  $1.49 \mu\text{g}/\text{m}^3$  –  $1.66 \mu\text{g}/\text{m}^3$ . BC predictions are highest in the Lower South district and lowest in the Central district. BC modeling was most effective in the Central, Lower Far Northeast, North, North Delaware, River Wards, and University Southwest planning districts, all of which have  $0.05 \mu\text{g}/\text{m}^3$  between predicted and measured values; in the Lower South district, the difference between predicted and measured BC concentrations is at its highest ( $0.12 \mu\text{g}/\text{m}^3$ ).

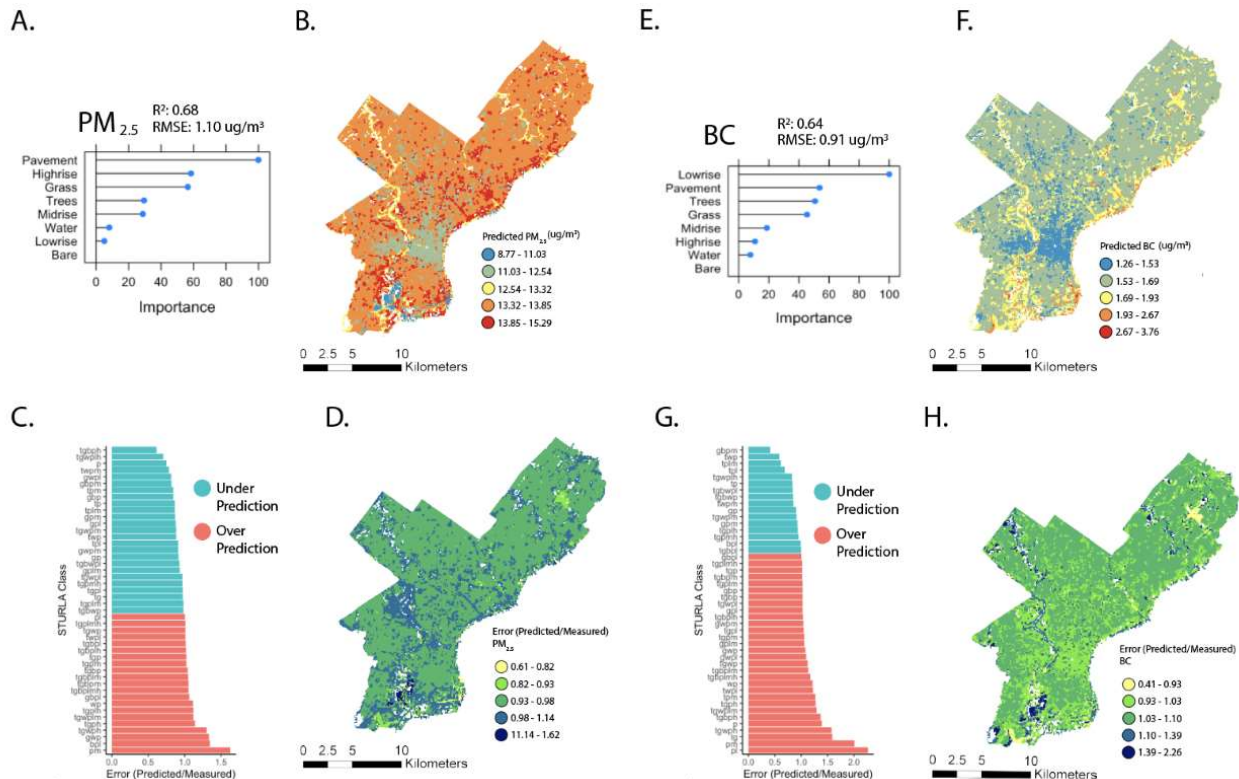


**Figure 5.** A.  $\text{PM}_{2.5}$  Random Forest Regression variable importance, correlation coefficient ( $R^2$ ) and error (RMSE). B. Predicted  $\text{PM}_{2.5}$  concentrations by quantile. C. Barplot of  $\text{PM}_{2.5}$  model error separated by STURLA class, with bar colors indicating underpredictions (blue) and overpredictions (red). D. Map of  $\text{PM}_{2.5}$  model validation error throughout Philadelphia. E. BC Random Forest Regression variable importance, correlation coefficient ( $R^2$ ) and error (RMSE). F. Predicted BC concentrations by quantile. G. Barplot of BC model error separated by STURLA class, with bar colors indicating underpredictions (blue) and overpredictions (red). H. Map of BC model validation error.

## 4.0 Discussion

### 4.1 Variation in $\text{PM}_{2.5}$ and BC by STURLA Class



PM<sub>2.5</sub> and BC varied by STURLA class (Figure 3), though most of the differences between classes are not statistically significant; no class had PM<sub>2.5</sub> concentrations or BC concentrations that were significantly different from all commonly sampled classes (Figure 4). Among the 14 most sampled STURLA classes, we find that the classes containing mid-rise and high-rise buildings hosted lower concentrations of PM<sub>2.5</sub> and BC relative to other commonly sampled classes; the five classes containing *m* or *h* (*tgplm*, *tgpm*, *tgplh*, *tgplmh*, and *tgbplm*) show the lowest average concentrations of PM<sub>2.5</sub> and BC (Figure 3). Four of these five classes (*tgpm*, *tgplh*, *tgplmh*, and *tgbplm*) also have the lowest daily variation in PM<sub>2.5</sub> concentrations, while all five have the lowest daily variation in BC concentrations (Figure 3). These results are unusual given the presence of taller buildings and relative lack of the natural environment; air pollutant concentrations tend to be higher in areas with a greater proportion of taller buildings (Aristodemou et al., 2018), while areas with a greater proportion of vegetation tend to have lower concentrations of air pollutants (Leung et al., 2011; Li et al., 2016). The taller buildings present in these classes can adversely impact wind flow and pollutant dispersal, causing an increase in pollutant concentrations closer to the peak of the building while decreasing concentrations at the ground-level where sampling occurred (Aristodemou et al., 2018; Zhang & Chu, 2013). Likewise, potential sources of PM and BC may simply be less abundant and/or smaller in magnitude where these classes are found, despite PM concentrations typically being higher in areas with denser built environment (Zhou & Lin, 2019). It is worth noting that classes with *m* and *h* components were generally sampled less frequently, except for *tgplm*, because they are less prevalent in the city's landscape. Some classes, such as *tgplh* and *tgplmh*, were not sampled enough to be able to quantify variability in pollutant concentrations on some days (Figure 3). Smaller sample sizes may have been less effective at capturing the full range of pollutant concentrations for specific classes than larger sample sizes.

While classes such as *tgbplm*, *tgplm*, and *tgplh*, are compositionally similar and have similar concentrations of PM<sub>2.5</sub> and BC (Figure 3), others display pronounced differences in pollutant levels despite compositional similarities with other STURLA classes. Among the most commonly sampled STURLA classes, *gpl* hosted the highest PM<sub>2.5</sub> concentrations and the third-highest BC concentrations. Class *gpl* is largely dominated by built environment, with roughly 89.9% of *gpl* land cover characterized by pavement and low-rise buildings (Figure 3). In class *tgplmh*, the class most similar to *gpl* by STURLA elements, we observe the second-lowest daily average PM<sub>2.5</sub> and BC concentrations throughout the sampling period. Conversely, class *gp*—also compositionally similar to *gpl*—hosted relatively high concentrations of PM<sub>2.5</sub> and BC just like *gpl*. In this class, we observe the third-highest daily average PM<sub>2.5</sub> concentration and second-highest daily average BC concentration. The differences in these classes may be explained by the differences in variety of urban landscape components present; *gp* and *gpl* classes lack the trees, mid-rise, and high-rise buildings that are present in the *tgplmh* class. Even though *gp* is considerably more vegetated than *tgplmh* (43.2% grass in *gp* vs. 17.8% trees/grass in *tgplmh*), class *gp* has pollutant concentrations that are closer to *gpl*, a class with 89.8% built environment. The high pollutant concentrations in *gp* and *gpl* suggest that grass does not facilitate a meaningful decrease in PM in urban environments, or at least in areas of the urban



environment that consist mostly of built environment. Trees may be more effective at attenuating air pollution than grass; most classes containing trees, with the exception of *tgwpl*, have lower concentrations of PM<sub>2.5</sub> and BC than *gp* and *gpl*. However, given the prevalence of classes with trees in Philadelphia, it is unclear whether it is the abundance of trees or the lack of built environment that contributes more to lower pollutant concentrations in these classes.

#### 4.2 Spatial Prediction of Air Pollution

As the most sampled STURLA classes generally do not have significantly different PM<sub>2.5</sub> and BC concentrations from other common classes (Figure 4), it is difficult to predict specific urban structure given just PM<sub>2.5</sub> and BC concentrations. However, the details of within class composition, or the proportion of STURLA components present in a given grid cell, can be used to predict PM pollutant concentrations despite heterogeneity in sources of PM and BC and sampling (e.g. on highways, near parks, stalled in traffic) and daily variation (Figure 3). Modeling was generally accurate for both PM<sub>2.5</sub> and BC; the largest difference between predicted and measured concentrations was 0.38 µg/m<sup>3</sup> for PM<sub>2.5</sub> and 0.12 µg/m<sup>3</sup> for BC (Table 1). Both models relied heavily on built environment to predict pollutant concentrations; pavement and high-rise were the most important STURLA components in modeling PM<sub>2.5</sub>, while low-rise and pavement were the most important components in modeling BC (Figure 5A, 5E). Pavement's importance in modeling the relationships between STURLA and PM is likely a function of the sampling design, which requires driving on roads throughout the sampling period, as well as the prevalence of pavement throughout Philadelphia. Vehicular emissions are a major contributor to PM emissions on roads (Cheng & Li, 2010), and developed areas in the urban environment are often in close proximity to facilities that generate PM pollution. The importance of low-rise buildings in BC modeling and the importance of high-rise buildings in PM<sub>2.5</sub> monitoring underscore the potential for buildings to influence pollutant concentrations; these buildings are not only positively associated with PM<sub>2.5</sub> and BC pollution, but their structure and organization throughout the urban environment can also influence local pollutant concentrations. Trees and grass are also relatively important in predicting pollutant concentrations, though not as important as the built components of the environment (Figure 5A, 5E). Trees and grass may be less important to the modeling due to their relative absence in urban environments, or because their presence in urban environments simply does not exert as strong an influence on pollutant concentrations.

Urban structure patterns did not contribute as much explanatory power for BC predictions as they did for PM<sub>2.5</sub> predictions; the relationship between urban structure and PM<sub>2.5</sub> has an  $R^2 = 0.68$ , while the relationship between urban structure and BC has an  $R^2 = 0.64$  (Figure 5). The lower correlation between BC and urban structure may be explained at least in part by the fact that BC is only a subset of PM<sub>2.5</sub>; PM<sub>2.5</sub> is inherently more abundant in the environment, as it has a greater variety of sources including vegetation, secondary aerosol formation from vehicular emissions (e.g. NO<sub>x</sub> and SO<sub>x</sub>) (Juda-Rezler et al., 2020), and suspension of crustal materials such as dust and soil (Querol et al., 2001). BC, in contrast, only comes from anthropogenic sources, and concentrations are largely influenced by road transport (Resquin et al., 2018). As a

result, BC has a slightly lower overall correlation to urban structure at large. These results suggest that sustainable urban planning focused on limiting exposure to air pollutants should focus on limiting built environment in favor of open spaces and natural environment to reduce potential sources of PM pollution, reduce variability in pollutant concentrations, and increase the capability of the urban environment to control pollutant levels. Vegetation specifically has been found to be instrumental in reducing PM concentrations (Escobedo & Nowak, 2009; Yin et al., 2011).

#### 4.3 Limitations

Though the sampling routes capture a sample of Philadelphia that is representative of the urban structure patterns prevalent in the city, the urban landscape can look quite different in other cities. As a result, some STURLA classes that are present or even abundant in other urban environments are not considered in these analyses. One such example is STURLA class *w*; though it is the sixth most common STURLA class in Philadelphia, we are unable to sample this class as it is impossible to drive through a cell containing only water. The accuracy of the prediction cannot be compared to measured values, as there are none; similar studies in the future should make appropriate adjustments to the experimental design to capture common classes that are otherwise inaccessible (i.e. classes without pavement). Though we include predictions and measurements for all classes with 2+ observations, we do not test for significant differences between classes with fewer than 20 unique sampled cells, nor do we examine how the compositions of these classes influence pollutant concentrations. Infrequently sampled classes constitute a fraction of the land cover/urban structure patterns present throughout Philadelphia, and in the absence of further sampling, it is difficult to accurately predict and characterize pollutant levels in these areas. Additionally, the use of STURLA is limited by the availability of up-to-date land cover and building height data; as the STURLA profile is based on data from 2017, it may not reflect changes in the Philadelphia's urban landscape that have occurred since then. Increased availability and accuracy of spatial data would make STURLA more effective in real time and would enable more accurate predictions.

#### 5.0 Conclusions

In this study, we explore the potential of STURLA as a way to simplify and meaningfully describe land cover and three-dimensional urban structure in the context of PM. Specifically, we sought to determine whether or not differences in particulate matter concentrations could be characterized by unique STURLA classifications, and explore the ability for different elements of land cover/urban structure to be used as predictors of PM concentrations. The class *tgbplm* was found to have the lowest PM<sub>2.5</sub> and BC concentrations, while *gpl* had the highest PM<sub>2.5</sub> concentrations ( $16.60 \pm 4.29 \mu\text{g}/\text{m}^3$ ) and *tgbwp* had the highest BC concentrations ( $2.31 \pm 1.94 \mu\text{g}/\text{m}^3$ ). While classes such as *gpl* and *tgbplm* had pollutant concentrations that stood out relative to other classes, we generally find a lack of significant differences between pollutant concentrations among classes, making it difficult to characterize urban structure

patterns based solely on concentrations of PM<sub>2.5</sub> and BC. However, we found that the components of STURLA and the proportions in which they are present are useful in predicting PM<sub>2.5</sub> and BC concentrations in different STURLA classes throughout the urban landscape. Of the STURLA components, components of the built environment (pavement, low-rise, high-rise) are the strongest predictors of urban PM<sub>2.5</sub> and BC pollution; low-rise buildings are more important in modeling BC than PM<sub>2.5</sub>, while the opposite is true for high-rise buildings. Vegetation components of the environment, such as trees and grass, have a fair amount of predictive power regarding PM<sub>2.5</sub> concentrations as well. The ability to approximate PM<sub>2.5</sub> concentrations using proportions of STURLA components suggests that careful consideration of land cover and urban structure patterns in planning can help cities to plan future development in a way that reduces potential exposure to air pollutants. STURLA may also be helpful in modeling relationships between urban structure and other prominent urban air pollutants of concern, such as ozone (O<sub>3</sub>), nitrogen oxides (NO<sub>x</sub>) and sulfur oxides (SO<sub>x</sub>). Further exploration of STURLA in the context of these other common urban air pollutants may reveal distinct differences between pollutant concentrations among STURLA classes that are not evident when looking solely at PM<sub>2.5</sub> and BC.

## References

- Abhijith, K. V., & Gokhale, S. (2015). Passive control potentials of trees and on-street parked cars in reduction of air pollution exposure in urban street canyons. *Environmental Pollution*, 204, 99–108. <https://doi.org/10.1016/j.envpol.2015.04.013>
- Anenberg, S. C., Henze, D. K., Tinney, V., Kinney, P. L., Raich W., Fann N., Malley, Chris S., Roman, H., Lamsal, L., Duncan B., Martin R. V., van Donkelaar, A., Brauer, M., Doherty, R., Jonson J. E., Davila, Y., Sudo Kengo, & Kuylensstierna, J. C. I. (2018). Estimates of the Global Burden of Ambient PM<sub>2.5</sub>, Ozone, and NO<sub>2</sub> on Asthma Incidence and Emergency Room Visits. *Environmental Health Perspectives*, 126(10), 107004. <https://doi.org/10.1289/EHP3766>
- Apte, J. S., Messier, K. P., Gani, S., Brauer, M., Kirchstetter, T. W., Lunden, M. M., Marshall, J. D., Portier, C. J., Vermeulen, R. C. H., & Hamburg, S. P. (2017). High-Resolution Air Pollution Mapping with Google Street View Cars: Exploiting Big Data. *Environmental Science & Technology*, 51(12), 6999–7008. <https://doi.org/10.1021/acs.est.7b00891>
- Aristodemou, E., Boganegra, L. M., Mottet, L., Pavlidis, D., Constantinou, A., Pain, C., Robins, A., & ApSimon, H. (2018). How tall buildings affect turbulent air flows and dispersion of pollution within a neighbourhood. *Environmental Pollution*, 233, 782–796. <https://doi.org/10.1016/j.envpol.2017.10.041>
- Baccarelli, A., Wright, R. O., Bollati, V., Tarantini, L., Litonjua, A. A., Suh, H. H., Zanobetti, A., Sparrow, D., Vokonas, P. S., & Schwartz, J. (2009). Rapid DNA Methylation Changes after Exposure to Traffic Particles. *American Journal of*

Respiratory and Critical Care Medicine, 179(7), 572–578.

<https://doi.org/10.1164/rccm.200807-1097OC>

Baldauf, R. W., Isakov, V., Deshmukh, P., Venkatram, A., Yang, B., & Zhang, K. M. (2016). Influence of solid noise barriers on near-road and on-road air quality.

Atmospheric Environment, 129, 265–276.

<https://doi.org/10.1016/j.atmosenv.2016.01.025>

Brantley, H. L., Hagler, G. S. W., Kimbrough, E. S., Williams, R. W., Mukerjee, S., & Neas, L. M. (2014). Mobile air monitoring data-processing strategies and effects on spatial air pollution trends. Atmospheric Measurement Techniques, 7(7), 2169–2183.

<https://doi.org/10.5194/amt-7-2169-2014>

Cadenasso, M. L., Pickett, S. T. A., & Schwarz, K. (2007). Spatial heterogeneity in urban ecosystems: Reconceptualizing land cover and a framework for classification.

Frontiers in Ecology and the Environment, 5(2), 80–88. [https://doi.org/10.1890/1540-9295\(2007\)5\[80:SHIUER\]2.0.CO;2](https://doi.org/10.1890/1540-9295(2007)5[80:SHIUER]2.0.CO;2)

Chen, L., Liu, C., Zou, R., Yang, M., & Zhang, Z. (2016). Experimental examination of effectiveness of vegetation as bio-filter of particulate matters in the urban environment. Environmental Pollution, 208, 198–208. <https://doi.org/10.1016/j.envpol.2015.09.006>

Cheng, Y.-H., & Li, Y.-S. (2010). Influences of Traffic Emissions and Meteorological Conditions on Ambient PM<sub>10</sub> and PM<sub>2.5</sub> Levels at a Highway Toll Station. Aerosol and Air Quality Research, 10(5), 456–462. <https://doi.org/10.4209/aaqr.2010.04.0025>

Cohen, A. J., Brauer, M., Burnett, R., Anderson, H. R., Frostad, J., Estep, K., Balakrishnan, K., Brunekreef, B., Dandona, L., Dandona, R., Feigin, V., Freedman, G., Hubbell, B., Jobling, A., Kan, H., Knibbs, L., Liu, Y., Martin, R., Morawska, L., ... Forouzanfar, M. H. (2017). Estimates and 25-year trends of the global burden of disease attributable to ambient air pollution: An analysis of data from the Global Burden of Diseases Study 2015. The Lancet, 389(10082), 1907–1918.

[https://doi.org/10.1016/S0140-6736\(17\)30505-6](https://doi.org/10.1016/S0140-6736(17)30505-6)

Collins, T. W., Grineski, S. E., & Morales, D. X. (2017a). Sexual Orientation, Gender, and Environmental Injustice: Unequal Carcinogenic Air Pollution Risks in Greater Houston. Annals of the American Association of Geographers, 107(1), 72–92.

<https://doi.org/10.1080/24694452.2016.1218270>

Collins, T. W., Grineski, S. E., & Morales, D. X. (2017b). Environmental injustice and sexual minority health disparities: A national study of inequitable health risks from air pollution among same-sex partners. Social Science & Medicine, 191, 38–47.

<https://doi.org/10.1016/j.socscimed.2017.08.040>

Cummings, L. E., Stewart, J. D., Reist, R., Shakya, K. M., Kremer, P (2020). Exploring the Spatiotemporal Variation of Air Pollution Throughout the Urban Landscape of Philadelphia, PA with Mobile Monitoring [Preprint]. Earth and Space Science Open

Archive; Earth and Space Science Open Archive.

<https://doi.org/10.1002/essoar.10503885.1>

Cyrys, J., Heinrich, J., Hoek, G., Meliefste, K., Lewné, M., Gehring, U., Bellander, T., Fischer, P., Vliet, P. van, Brauer, M., Wichmann, H.-E., & Brunekreef, B. (2003). Comparison between different traffic-related particle indicators: Elemental carbon (EC), PM 2.5 mass, and absorbance. *Journal of Exposure Science & Environmental Epidemiology*, 13(2), 134–143. <https://doi.org/10.1038/sj.jea.7500262>

deSouza, P., Anjomshoaa, A., Duarte, F., Kahn, R., Kumar, P., & Ratti, C. (2020). Air quality monitoring using mobile low-cost sensors mounted on trash-trucks: Methods development and lessons learned. *Sustainable Cities and Society*, 60, 102239. <https://doi.org/10.1016/j.scs.2020.102239>

Deville Cavellin, L., Weichenthal, S., Tack, R., Ragettli, M. S., Smargiassi, A., & Hatzopoulou, M. (2016). Investigating the Use Of Portable Air Pollution Sensors to Capture the Spatial Variability Of Traffic-Related Air Pollution. *Environmental Science & Technology*, 50(1), 313–320. <https://doi.org/10.1021/acs.est.5b04235>

Diaz Resquin, M., Santágata, D., Gallardo, L., Gómez, D., Rössler, C., & Dawidowski, L. (2018). Local and remote black carbon sources in the Metropolitan Area of Buenos Aires. *Atmospheric Environment*, 182, 105–114. <https://doi.org/10.1016/j.atmosenv.2018.03.018>

Dockery, D. W., Pope, C. A., Xu, X., Spengler, J. D., Ware, J. H., Fay, M. E., Ferris, B. G., & Speizer, F. E. (1993). An Association between Air Pollution and Mortality in Six U.S. Cities. *New England Journal of Medicine*, 329(24), 1753–1759. <https://doi.org/10.1056/NEJM199312093292401>

Eeftens, M., Beelen, R., de Hoogh, K., Bellander, T., Cesaroni, G., Cirach, M., Declercq, C., Dèdelè, A., Dons, E., de Nazelle, A., Dimakopoulou, K., Eriksen, K., Falq, G., Fischer, P., Galassi, C., Gražulevičienė, R., Heinrich, J., Hoffmann, B., Jerrett, M., ... Hoek, G. (2012). Development of Land Use Regression Models for PM<sub>2.5</sub>, PM<sub>2.5</sub> Absorbance, PM<sub>10</sub> and PM<sub>coarse</sub> in 20 European Study Areas; Results of the ESCAPE Project. *Environmental Science & Technology*, 46(20), 11195–11205. <https://doi.org/10.1021/es301948k>

Eisenman, T. S., Churkina, G., Jariwala, S. P., Kumar, P., Lovasi, G. S., Pataki, D. E., Weinberger, K. R., & Whitlow, T. H. (2019). Urban trees, air quality, and asthma: An interdisciplinary review. *Landscape and Urban Planning*, 187(February), 47–59. <https://doi.org/10.1016/j.landurbplan.2019.02.010>

Escobedo, F. J., & Nowak, D. J. (2009). Spatial heterogeneity and air pollution removal by an urban forest. *Landscape and Urban Planning*, 90(3), 102–110. <https://doi.org/10.1016/j.landurbplan.2008.10.021>



Gallagher, J., Baldauf, R., Fuller, C. H., Kumar, P., Gill, L. W., & McNabola, A. (2015). Passive methods for improving air quality in the built environment: A review of porous and solid barriers. *Atmospheric Environment*, 120, 61–70.  
<https://doi.org/10.1016/j.atmosenv.2015.08.075>

Gray, S. C., Edwards, S. E., & Miranda, M. L. (2013). Race, socioeconomic status, and air pollution exposure in North Carolina. *Environmental Research*, 126, 152–158.  
<https://doi.org/10.1016/j.envres.2013.06.005>

Hagler, G. S. W., Lin, M. Y., Khlystov, A., Baldauf, R. W., Isakov, V., Faircloth, J., & Jackson, L. E. (2012). Field investigation of roadside vegetative and structural barrier impact on near-road ultrafine particle concentrations under a variety of wind conditions. *Science of the Total Environment*, 419, 7–15.  
<https://doi.org/10.1016/j.scitotenv.2011.12.002>

Halonen, J. I., Lanki, T., Yli-Tuomi, T., Kulmala, M., Tiittanen, P., & Pekkanen, J. (2008). Urban air pollution, and asthma and COPD hospital emergency room visits. *Thorax*, 63(7), 635–641. <https://doi.org/10.1136/thx.2007.091371>

Hamra, G. B., Guha, N., Cohen, A., Laden, F., Raaschou-Nielsen, O., Samet, J. M., Vineis, P., Forastiere, F., Saldiva, P., Yorifuji, T., & Loomis, D. (2014). Outdoor particulate matter exposure and lung cancer: A systematic review and meta-analysis. *Environmental Health Perspectives*, 122(9), 906–911.  
<https://doi.org/10.1289/ehp/1408092>

Hamstead, Z. A., Kremer, P., Larondelle, N., McPhearson, T., & Haase, D. (2016). Classification of the heterogeneous structure of urban landscapes (STURLA) as an indicator of landscape function applied to surface temperature in New York City. *Ecological Indicators*, 70, 574–585. <https://doi.org/10.1016/j.ecolind.2015.10.014>

Han, L., Zhou, W., Li, W., & Li, L. (2014). Impact of urbanization level on urban air quality: A case of fine particles (PM<sub>2.5</sub>) in Chinese cities. *Environmental Pollution*, 194, 163–170. <https://doi.org/10.1016/j.envpol.2014.07.022>

Hervé, M. (2021). RVAideMemoire: Testing and Plotting Procedures for Biostatistics (0.9-79) [Computer software]. <https://CRAN.R-project.org/package=RVAideMemoire>

Hitzenberger, R., & Tohno, S. (2001). Comparison of black carbon (BC) aerosols in two urban areas – concentrations and size distributions. *Atmospheric Environment*, 35(12), 2153–2167. [https://doi.org/10.1016/S1352-2310\(00\)00480-5](https://doi.org/10.1016/S1352-2310(00)00480-5)

Honda, A., Fukushima, W., Oishi, M., Tsuji, K., Sawahara, T., Hayashi, T., Kudo, H., Kashima, Y., Takahashi, K., Sasaki, H., Ueda, K., & Takano, H. (2017). Effects of Components of PM<sub>2.5</sub> Collected in Japan on the Respiratory and Immune Systems. *International Journal of Toxicology*, 36(2), 153–164.  
<https://doi.org/10.1177/1091581816682224>

Hu, H., Wu, J., Li, Q., Asweto, C., Feng, L., Yang, X., Duan, F., Duan, J., & Sun, Z. (2016). Fine particulate matter induces vascular endothelial activation via IL-6 dependent JAK1/STAT3 signaling pathway. *Toxicology Research*, 5(3), 946–953. <https://doi.org/10.1039/c5tx00351b>

Ihaka, R., & Gentleman, R. (1996). R: A Language for Data Analysis and Graphics. *Journal of Computational and Graphical Statistics*, 5(3), 299–314. <https://doi.org/10.1080/10618600.1996.10474713>

Juda-Rezler, K., Reizer, M., Maciejewska, K., Błaszczak, B., & Klejnowski, K. (2020). Characterization of atmospheric PM<sub>2.5</sub> sources at a Central European urban background site. *Science of The Total Environment*, 713, 136729. <https://doi.org/10.1016/j.scitotenv.2020.136729>

Kremer, P., Larondelle, N., Zhang, Y., Pasles, E., & Haase, D. (2018). Within-class and neighborhood effects on the relationship between composite urban classes and surface temperature. *Sustainability (Switzerland)*, 10(3). <https://doi.org/10.3390/su10030645>

Kuhn, M. (2008). Building Predictive Models in R Using the caret Package. *Journal of Statistical Software*, 28(1), 1–26. <https://doi.org/10.18637/jss.v028.i05>

Larondelle, N., Hamstead, Z. A., Kremer, P., Haase, D., & McPhearson, T. (2014). Applying a novel urban structure classification to compare the relationships of urban structure and surface temperature in Berlin and New York City. *Applied Geography*, 53, 427–437. <https://doi.org/10.1016/j.apgeog.2014.07.004>

Leung, D. Y. C., Tsui, J. K. Y., Chen, F., Yip, W.-K., Vrijmoed, L. L. P., & Liu, C.-H. (2011). Effects of Urban Vegetation on Urban Air Quality. *Landscape Research*, 36(2), 173–188. <https://doi.org/10.1080/01426397.2010.547570>

Liu, H., Zhang, X., Zhang, H., Yao, X., Zhou, M., Wang, J., He, Z., Zhang, H., Lou, L., Mao, W., Zheng, P., & Hu, B. (2018). Effect of air pollution on the total bacteria and pathogenic bacteria in different sizes of particulate matter. *Environmental Pollution*, 233, 483–493. <https://doi.org/10.1016/j.envpol.2017.10.070>

Mitz, E., Kremer, P., Larondelle, N., & Stewart, J. (2020). Structure of Urban Landscape and Surface Temperature: A Case Study in Philadelphia, PA [Preprint]. *Earth and Space Science Open Archive*; Earth and Space Science Open Archive. <https://doi.org/10.1002/essoar.10503832.1>

Nemitz, E., Vieno, M., Carnell, E., Fitch, A., Steadman, C., Cryle, P., Holland, M., Morton, R. D., Hall, J., Mills, G., Hayes, F., Dickie, I., Carruthers, D., Fowler, D., Reis, S., & Jones, L. (2020). Potential and limitation of air pollution mitigation by vegetation and uncertainties of deposition-based evaluations. *Philosophical Transactions of the Royal Society A: Mathematical, Physical and Engineering Sciences*, 378(2183), 20190320. <https://doi.org/10.1098/rsta.2019.0320>

Ng, W. Y., & Chau, C. K. (2012). Evaluating the role of vegetation on the ventilation performance in isolated deep street canyons. *International Journal of Environment and Pollution*, 50(1–4), 98–110. <https://doi.org/10.1504/IJEP.2012.051184>

Oliveira, S., Oehler, F., San-Miguel-Ayanz, J., Camia, A., & Pereira, J. M. C. (2012). Modeling spatial patterns of fire occurrence in Mediterranean Europe using Multiple Regression and Random Forest. *Forest Ecology and Management*, 275, 117–129. <https://doi.org/10.1016/j.foreco.2012.03.003>

Paul, G., Nolen, J. E., Alexander, L., Bender, L. K., Vleet, V., Barrett, W., Jump, Z., Rappaport, S., Samet, J. M., Ballentine, N., Nimirowski, T., Innocenzi, L., Wojs, V., Lavelle, L., Clark, C., Fitzgerald, J., Eyer, A., Lacina, K., Macmunn, A., ... Designs, O. (2019). State of the Air 2019. [www.stateoftheair.org](http://www.stateoftheair.org)

Perlin, S. A., Sexton, K., & Wong, D. W. S. (1999). An examination of race and poverty for populations living near industrial sources of air pollution. *Journal of Exposure Science & Environmental Epidemiology*, 9(1), 29–48. <https://doi.org/10.1038/sj.jea.7500024>

Pope III, C. A., Burnett, R. T., Thun, M. J., Calle, E. E., Krewski, D., Ito, K., & Thurston, G. D. (2002). Lung Cancer, Cardiopulmonary Mortality, and Long-term Exposure to Fine Particulate Air Pollution. *JAMA*, 287(9), 1132–1141. <https://doi.org/10.1001/jama.287.9.1132>

Querol, X., Alastuey, A., Rodriguez, S., Plana, F., Ruiz, C. R., Cots, N., Massagué, G., & Puig, O. (2001). PM10 and PM2.5 source apportionment in the Barcelona Metropolitan area, Catalonia, Spain. *Atmospheric Environment*, 35(36), 6407–6419. [https://doi.org/10.1016/S1352-2310\(01\)00361-2](https://doi.org/10.1016/S1352-2310(01)00361-2)

Rabinovitch, N., Strand, M., & Gelfand, E. W. (2006). Particulate levels are associated with early asthma worsening in children with persistent disease. *American Journal of Respiratory and Critical Care Medicine*, 173(10), 1098–1105. <https://doi.org/10.1164/rccm.200509-1393OC>

Diaz Resquin, M., Santágata, D., Gallardo, L., Gómez, D., Rössler, C., & Dawidowski, L. (2018). Local and remote black carbon sources in the Metropolitan Area of Buenos Aires. *Atmospheric Environment*, 182, 105–114. <https://doi.org/10.1016/j.atmosenv.2018.03.018>

Saraswat, A., Apte, J. S., Kandlikar, M., Brauer, M., Henderson, S. B., & Marshall, J. D. (2013). Spatiotemporal Land Use Regression Models of Fine, Ultrafine, and Black Carbon Particulate Matter in New Delhi, India. *Environmental Science & Technology*, 47(22), 12903–12911. <https://doi.org/10.1021/es401489h>

Shakya, K. M., Kremer, P., Henderson, K., McMahon, M., Peltier, R. E., Bromberg, S., & Stewart, J. (2019). Mobile monitoring of air and noise pollution in Philadelphia neighborhoods during summer 2017. *Environ. Pollut.*, 255(Pt 1), 113195–113195. <https://doi.org/10.1016/j.envpol.2019.113195>

Shakya, K. M., Rupakheti, M., Aryal, K., & Peltier, R. E. (2016). Respiratory Effects of High Levels of Particulate Exposure in a Cohort of Traffic Police in Kathmandu, Nepal. *Journal of Occupational and Environmental Medicine*, 58(6), e218. <https://doi.org/10.1097/JOM.0000000000000753>

Shi, Y., Zhao, T., Yang, X., Sun, B., Li, Y., Duan, J., & Sun, Z. (2019). PM2.5-induced alteration of DNA methylation and RNA-transcription are associated with inflammatory response and lung injury. *Science of The Total Environment*, 650, 908–921. <https://doi.org/10.1016/j.scitotenv.2018.09.085>

Sm, S. N., Reddy Yasa, P., Mv, N., Khadirnaikar, S., & Pooja Rani. (2019). Mobile monitoring of air pollution using low cost sensors to visualize spatio-temporal variation of pollutants at urban hotspots. *Sustainable Cities and Society*, 44, 520–535. <https://doi.org/10.1016/j.scs.2018.10.006>

Sørensen, M., Autrup, H., Hertel, O., Wallin, H., Knudsen, L. E., & Loft, S. (2003). Personal exposure to PM2.5 and biomarkers of DNA damage. *Cancer Epidemiology, Biomarkers & Prevention: A Publication of the American Association for Cancer Research*, Cosponsored by the American Society of Preventive Oncology, 12(3), 191–196.

Stewart, J. D., Kremer, P., Shakya, K. M., Conway, M., & Saad, A. (2021). Outdoor Atmospheric Microbial Diversity Is Associated With Urban Landscape Structure and Differs From Indoor-Transit Systems as Revealed by Mobile Monitoring and Three-Dimensional Spatial Analysis. *Frontiers in Ecology and Evolution*, 9. <https://doi.org/10.3389/fevo.2021.620461>

Stewart, J. D., Shakya, K. M., Bilinski, T., Wilson, J. W., Ravi, S., & Choi, C. S. (2020). Variation of near surface atmosphere microbial communities at an urban and a suburban site in Philadelphia, PA, USA. *Science of The Total Environment*, 724, 138353. <https://doi.org/10.1016/j.scitotenv.2020.138353>

Targino, A. C., Gibson, M., Krecl, P., Rodrigues, M. V., Santos, M. M. D., & Corrêa, M. de P. (2016). Hotspots of black carbon and PM2.5 in an urban area and relationships to traffic characteristics. *Environmental Pollution*, 218, 475–486. <https://doi.org/10.1016/j.envpol.2016.07.027>

United Nations, Department of Economic and Social Affairs, Population Division (2019). *World Urbanization Prospects: The 2018 Revision*. New York: United Nations.

Van den Bossche, J., Peters, J., Verwaeren, J., Botteldooren, D., Theunis, J., & De Baets, B. (2015). Mobile monitoring for mapping spatial variation in urban air quality: Development and validation of a methodology based on an extensive dataset. *Atmospheric Environment*, 105, 148–161.  
<https://doi.org/10.1016/j.atmosenv.2015.01.017>

Van Poppel, M., Peters, J., & Bleux, N. (2013). Methodology for setup and data processing of mobile air quality measurements to assess the spatial variability of concentrations in urban environments. *Environmental Pollution*, 183, 224–233.  
<https://doi.org/10.1016/j.envpol.2013.02.020>

World Health Organization (2018). 9 out of 10 people worldwide breathe polluted air, but more countries are taking action. News release, Geneva.  
<https://www.who.int/news/item/02-05-2018-9-out-of-10-people-worldwide-breathe-polluted-air-but-more-countries-are-taking-action>

Xing, Y., & Brimblecombe, P. (2019). Role of vegetation in deposition and dispersion of air pollution in urban parks. *Atmospheric Environment*, 201(December 2018), 73–83.  
<https://doi.org/10.1016/j.atmosenv.2018.12.027>

Yin, S., Shen, Z., Zhou, P., Zou, X., Che, S., & Wang, W. (2011). Quantifying air pollution attenuation within urban parks: An experimental approach in Shanghai, China. *Environmental Pollution*, 159(8), 2155–2163.  
<https://doi.org/10.1016/j.envpol.2011.03.009>

Yuan, M., Song, Y., Huang, Y., Shen, H., & Li, T. (2019). Exploring the association between the built environment and remotely sensed PM<sub>2.5</sub> concentrations in urban areas. *Journal of Cleaner Production*, 220, 1014–1023.  
<https://doi.org/10.1016/j.jclepro.2019.02.236>

Zelikoff, J. T., Chen, L. C., Cohen, M. D., Fang, K., Gordon, T., Li, Y., Nadziejko, C., & Schlesinger, R. B. (2003). Effects of Inhaled Ambient Particulate Matter on Pulmonary Antimicrobial Immune Defense. *Inhalation Toxicology*, 15(2), 131–150.  
<https://doi.org/10.1080/089583703004478>

Zhang, A., Qi, Q., Jiang, L., Zhou, F., & Wang, J. (2013). Population Exposure to PM<sub>2.5</sub> in the Urban Area of Beijing. *PLOS ONE*, 8(5), e63486.  
<https://doi.org/10.1371/journal.pone.0063486>

Zhou, S., & Lin, R. (2019). Spatial-temporal heterogeneity of air pollution: The relationship between built environment and on-road PM<sub>2.5</sub> at micro scale. *Transportation Research Part D: Transport and Environment*, 76, 305–322.  
<https://doi.org/10.1016/j.trd.2019.09.004>

Zhou, Z., Dionisio, K. L., Arku, R. E., Quaye, A., Hughes, A. F., Vallarino, J., Spengler, J. D., Hill, A., Agyei-Mensah, S., & Ezzati, M. (2011). Household and community



poverty, biomass use, and air pollution in Accra, Ghana. Proceedings of the National Academy of Sciences, 108(27), 11028–11033.

<https://doi.org/10.1073/pnas.1019183108>

Zhu, Y., Xie, J., Huang, F., & Cao, L. (2020). Association between short-term exposure to air pollution and COVID-19 infection: Evidence from China. Science of The Total Environment, 727, 138704. <https://doi.org/10.1016/j.scitotenv.2020.138704>